Modeling of MEMS Thermal Actuation with External Heat Source

J. Varona[1], M. Tecpoyotl-Torres[1], A. A. Hamoui[2]
[1]*Centro de Investigación en Ingeniería y Ciencias Aplicadas, UAEM, México*
[2]*Department of Electrical and Computer Engineering, McGill University, Canada*
varona@ieee.org

Abstract

This paper presents the thermal analysis and design of micro-actuators based on standard MEMS technology irrespective of the input heat source. The typical approach for driving this kind of actuators is by applying an electric current that flows through the device and generates Joule heating. However, this requires relatively large currents and the corresponding power consumption. As an alternative to electrically driven thermal actuators, this work explores the possibility of developing thermal actuators that can be activated with an external heat source and, for example, scavenge heat from the surrounding medium. The mathematical description for heat transfer within the MEMS device is presented along with numerical simulation results. A discussion about the opportunities and limitations of externally heated thermo actuators is also presented.

1. Introduction

Micro-Electro-Mechanical Systems (MEMS) offer the possibility of reducing entire complex engineering systems to the micro-scale domain. The integration of electronic circuitry and MEMS sensor-actuator devices results in an unprecedented overall reduction in size and mass beyond the capabilities of any previous technology.

However, one of the limiting factors that prevent many microsystems from being practically implemented is the lack of an enabling power supply unit that may be integrated within the system. With present technology, energy must be supplied from external bulky batteries that are several times the size of the microsystem itself. As conventional batteries do not scale-down well, several approaches for developing micro power sources are being investigated. Among the different technologies being studied to obtain a suitable micro-battery are miniature and micro-combustors, radioisotope based generators, etc. [1, 2, 3].

Some researchers [3] already agree that the most viable power supply strategy for autonomous MEMS (those unattached to an external power supply unit) is the one comprising energy harvesting from the environment and on-board energy storage elements.

Accordingly, this works presents a study towards developing MEMS actuators that can operate autonomously by exploiting a thermal gradient in the surrounding environment. Such conditions in which a high heat density is available are fairly common in many practical situations where MEMS are generally found, for example sensors in the automotive and aerospace industry and in every application using a microprocessor or other electronic circuitry that dissipates relatively large amounts of heat.

The future goal is to make productive use of the high heat density available transforming the thermal energy into a more useful form of energy while dissipating the heat in the process.

2. Background

A number of thermal actuators have been previously investigated both analytically and experimentally [4-9]. Traditional thermal actuators are electrically driven and heat is generated in accordance with the Lenz-Joule law.

Among the most well documented thermal actuators is the single hot-arm [4, 5] illustrated in Figure 1.

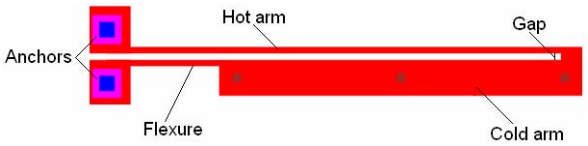

Figure 1. Standard single hot-arm thermal actuator.

0-7695-2974-7/07 $25.00 © 2007 IEEE
DOI 10.1109/CERMA.2007.60

This actuator is comprised of two asymmetric microbeams (arms) connected in series and fixed to the substrate at the anchors. When a constant voltage is applied across the two anchor pads, corresponding electrical current flows through the arms. The larger current density in the narrower hot arm leads to a higher temperature compared to that in the wide or cold arm. The differential thermal expansion generates a deflecting force towards the cold arm.

Although the single hot-arm device offers relatively large deflection and force, it suffers from poor power efficiency as the heat generated in the cold arm does not contribute to the intended motion of the actuator. To circumvent this and other design limitations, work has been done to develop an improved double-hot-arm electrothermal actuator [6] like the one sketched in Figure 2.

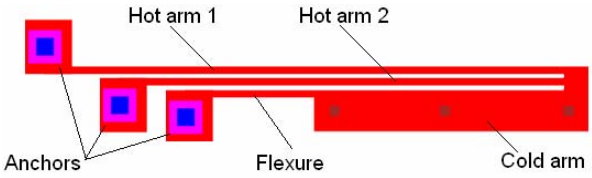

Figure 2. Schematic of a two-hot-arm thermal actuator.

In the two-hot arm device, the electric current is forced through the two thin hot-arms only and the cold arm is no longer part of the electric circuit. In this manner, all the heat that is generated contributes to the motion of the actuator considerably increasing its power efficiency.

Other electrothermal devices have been demonstrated on the microscale. The vertical thermal actuator analyzed in [7, 8] can provide large force and deflection perpendicular to the substrate. Other popular thermal actuator, known as chevron due to its "v" shape, is studied in [9].

The proposal of this work is to eliminate the need for the electric power supply unit and directly utilize a heat source that might be already present in the surrounding environment to power the MEMS thermal actuators. The analytical and numerical results for this approach are presented in the following sections.

3. Modeling

3.1. Thermal Analysis

The fundamental equation that describes the three dimensional heat transfer problem is the so called heat diffusion equation:

$$\nabla^2 T + \frac{q}{k} = \frac{1}{\alpha}\frac{\partial T}{\partial t} \qquad (1)$$

where $\nabla^2 T = \frac{\partial^2 T}{\partial x^2} + \frac{\partial^2 T}{\partial y^2} + \frac{\partial^2 T}{\partial z^2}$ and $\alpha = \frac{k}{\rho c}$. T is the temperature distribution, α is known as the thermal diffusivity, k is the thermal conductivity of the material, ρ represents the density, c is the specific heat capacity, and q accounts for a volumetric heat release.

For undertaking the thermal analysis, the standard single hot-arm device is used as example. Hot-arms are usually fabricated with surface micromachining technology [10] that is compatible with IC technology. Figure 3 presents the cross-section view of the actuator's structure showing the different layers and materials commonly employed for its fabrication.

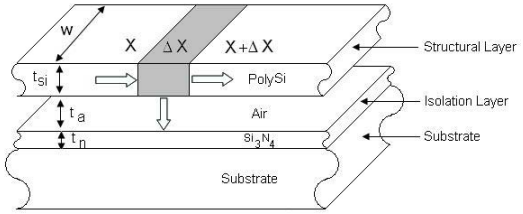

Figure 3. Cross-sectional view of one section of the hot-arm thermal actuator.

The partial differential heat diffusion equation given in (1) may be fairly simplified by employing some reasonable assumptions. At first, considering that the length of the actuator is much larger than the size of its cross section, the electrothermal analysis is generally treated as a one-dimensional problem [4]. Secondly, as the device is externally heated at one end, there is no heat generation within the element and equation (1) reduces to an ordinary differential equation in the form of:

$$\frac{d^2 T}{dx^2} = \frac{1}{\alpha}\frac{dT}{dt} \qquad (2)$$

3.2. Temperature Distribution

Considering that the operating temperatures for this kind of actuators are relatively low, the radiation effect can be neglected [4, 7]. The steady-state thermal analysis can be derived from examining a differential element of the hot-arm structure of width w, thickness t and length Δx as illustrated in Figure 4. Following the First Law of Thermodynamics:

$$-kwt\left.\frac{dT}{dx}\right|_x = -kwt\left.\frac{dT}{dx}\right|_{x+\Delta x} + hw(T - T_a)\Delta x \qquad (3)$$

where k is the thermal conductivity of the structural material, T is the operating temperature, T_a is the

ambient temperature, and h is the convection coefficient that accounts for the effect of heat transfer to the ambient.

After re-arranging equation (3) and taking the limit as $\Delta x \to 0$, the following second-order differential equation is obtained:

$$\frac{d^2T}{dx^2} - \frac{h}{kt}(T - T_a) = 0 \qquad (4)$$

If changing variables in the form of $\theta = T - T_a$ and $B = \sqrt{\frac{h}{kt}}$, the general solution for equation (4) is:

$$T_{(x)} = T_s + C_1 e^{Bx} + C_2 e^{-Bx} \qquad (5)$$

A particular solution for boundary conditions $\theta_{(0)} = \theta_2$ and $\theta_{(L)} = 0$ yields:

$$C_1 = \frac{\theta_2}{1 - e^{2BL}}, \; C_2 = \theta_2 - C_1 \qquad (6)$$

Based on equations (5) and (6), Figure 4 presents an example for the thermal distribution along the beams of a single hot-arm with a total length of 420μm. The effect of the exact value of the convection coefficient h on the temperature profile can be observed as the distribution changes from a linear to exponential shape.

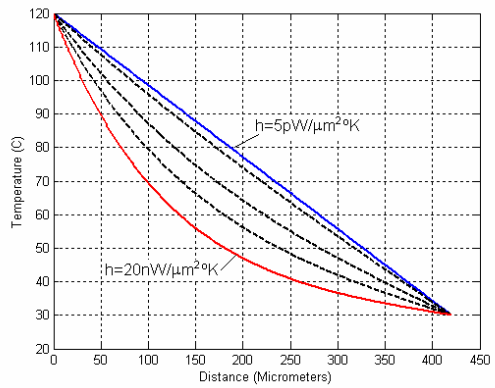

Figure 4. Solution for temperature distribution along the actuator arms for different values of the convection coefficient h.

The results given in Figure 4 assume that one of the anchors is at ambient temperature of 30°C and the other one is brought to 120°C via an external heat source. The width of the two arms was taken equal.

External heat sources exceeding temperatures in the order of 100°C are fairly common in environments where MEMS find practical use. Examples include automotive and aerospace industry where high heat transfer rates and temperatures well beyond 500°C are commonly available [11]. Another potential widespread source of heat for MEMS is found in modern electronic VLSI integrated circuits that may have power densities in excess of 40W/cm^2 [12, 13].

To estimate the maximum temperature that can be reached as a function of the heat flux Q applied at an anchor pad, one can start from:

$$Q = \frac{\Delta T}{R_t}; \Rightarrow \Delta T = QR_t \qquad (7)$$

where Q is the heat transfer rate, ΔT represents the change in temperature or gradient, R_t is the interfacial conductance or thermal resistance that accounts for heat (energy) leakage from the outside surface of the beam to the substrate according to:

$$R_t = \frac{S}{A}\left[\frac{t_{si}}{k_p} + \frac{t_a}{k_v} + \frac{t_n}{k_n}\right] \qquad (8)$$

where A is the cross-sectional area of the polysilicon beam; t_{si}, t_a and t_n are the thickness of the polysilicon, air and nitride layers in a standard surface micromachining process; k_p, k_v and k_n are the corresponding thermal conductivity values for each of the material layers; and S is the conduction shape factor that depends on the geometry of the element, roughness, etc.

For the particular case under study, we recall equations (6) and (7) and since C1<<C2 it also follows that:

$$\Delta T_{(x)} \approx C_2 e^{-Bx} \qquad (9)$$

Taking q=Q/A as the heat rate per unit area, and combining equations (7) and (9):

$$qAR_t \approx \theta_2 e^{-Bx} \qquad (10)$$

Thus, at the anchor pad we have:

$$\frac{qAR_t}{e^{-Bx}} \approx \theta_2 = T_{(x=0)} - T_s \qquad (11)$$

Figure 5 shows the anchor temperature as a function of the applied heat transfer rate q, for usual values of heat density found in present-day VLSI chips.

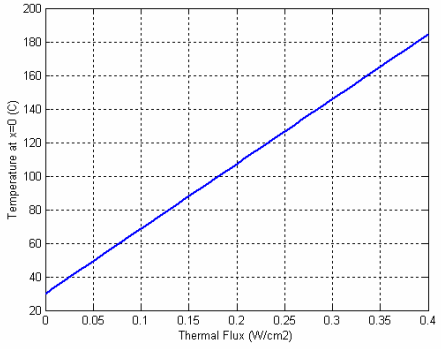

Figure 5. Temperature as a function of the heat flux per unit area applied at the anchor pad.

3.3. Thermal Expansion

The linear thermal expansion ΔL is given by the following set of equations:

$$\Delta L = K^{-1} F_{thermal},\ F_{thermal} = A\sigma,\ \sigma = E\alpha\Delta T \quad (13)$$

where K is the stiffness coefficient, A is the cross-sectional area, E corresponds to the Young's Modulus, $\Delta T=(T-T_a)$, σ represents the thermal stress and α is the thermal expansion coefficient of the material.

The thermal expansion for each of the two arms is obtained by integrating along the beam structure:

$$\Delta L = \alpha \int_0^L (T - T_a)dx \quad (14)$$

and substituting the appropriate temperature distribution from equation (5) yields:

$$\Delta L = \alpha \int_0^L (C_1 e^{Bx} + C_2 e^{-Bx})dx \quad (15)$$

Finally, the mechanical deflection of the actuator can be estimated based on the thermal expansion by using some of the well established structural engineering methods presented in [5, 7] that analyze the bending moments acting on the hot-arm by solving a set of simultaneous equations.

3.4. Transient Analysis

Owing to its complexity, the dynamic response of micromechanical devices is often determined experimentally and then related to the static analytical model. Even for numerical simulators and CAD tools the computational cost of calculating transient behaviors is very expensive due to the large number of nodes in the 3-D finite-element-model of the actuators.

As an approach to estimate the performance of the actuator before actual fabrication, a dynamic system model can be formulated based on the principles of thermodynamics and heat transfer theory.

At first we consider the cooling transient where the element is subject to convective cooling. The First Law of Thermodynamics for a closed system states that the heat transfer rate Q is equal to the change of the internal thermal energy U with time:

$$Q = \frac{dU}{dt} \quad (16)$$

As the object is being convectively cooled, the above equation may be expressed in the form of:

$$\bar{h}A(T - T_\infty) = \frac{d}{dt}\left[\rho c V (T - T_{ref})\right] \quad (17)$$

where $\bar{h}$ is the average convection coefficient over the surface, A is the cross-sectional area, ρ is the density of the material, V is the volume, c is the specific heat capacity of the material and T_{ref} is an arbitrary temperature at which U is defined equal to zero.

Thus, the general solution for (17) is:

$$\ln(T - T_\infty) = -\frac{t}{(\rho c V / \bar{h}A)} + C \quad (18)$$

where the group $(\rho c V / \bar{h}A)$ is the time constant τ.

If using the initial temperature condition T(t=0)=Ti, the value of the integration constant in equation (18) is $C = \ln(T_i - T_\infty)$, and the cooling of the object is:

$$T(t) = T_\infty + (T_i - T_\infty)e^{-t/\tau} \quad (19)$$

Note that the thermal conductivity is not considered in the equations above as it was assumed to be irrelevant in the cooling process. As the thickness of the beams is small compared to the length of the arms it is safe to assume that the temperature along the thickness of the beams is uniform and thus internal conduction is not important. One criterion that is used in convective analysis to verify the legitimacy of this assumption consists on checking that the Biot number meets the condition Bi<<1, where $Bi = \frac{\bar{h} \cdot t_{si}}{k_p}$.

The result corresponding to the cooling transient under natural convection is plotted in Figure 6.

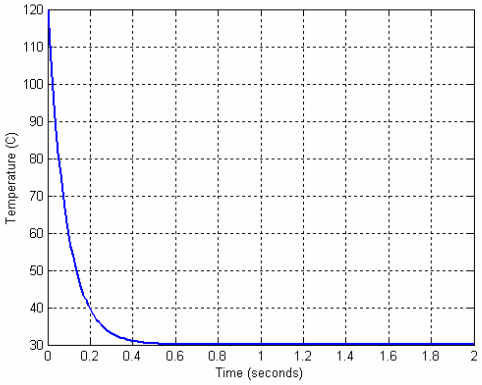

Figure 6. Estimated cooling transient of the hot-arm actuator.

The analogous dependence can be expressed for heating transient behavior when the heat is transferred by conduction. The analytical solution for heating transient is defined by:

$$T(t) = T_s + qAR_t(1 - e^{-t/\tau}) \quad (21)$$

where R_t and τ are the thermal resistance and the time constant respectively described by

$$R_t = \frac{S}{A}\left[\frac{t_{si}}{k_p} + \frac{t_a}{k_v} + \frac{t_n}{k_n}\right] \text{ and } \tau = \frac{\rho c V}{\bar{h}kA}(\bar{h}Lt + k).$$

Figure 7(a) illustrates the total time response of the actuator composed by the time required for heating and cooling. Also, as can be observed in Figure 7(b), the maximum frequency of operation can be increased if a bias temperature is used. This bias temperature is such that the deflection of the actuator due to thermal expansion at this point is negligible and the actuator does not need to cool down below this level before starting a new heating cycle.

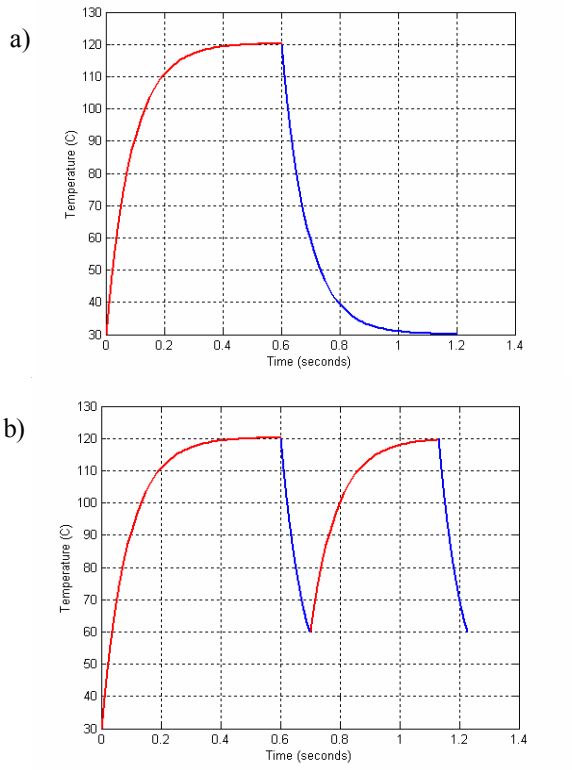

Figure 7. (a) Total time response for one full cycle. (b) Maximum operating frequency if a bias temperature is defined.

4. Design Issues

As described in section 3, the model assumes that heat is applied on top of one of the anchors while the other one remains cold attached to the substrate at room temperature. Another possibility is to have a hot substrate heating both anchors equally and then obtain deflection by differential thermal expansion using asymmetric arms. For a cyclical operation, the latter approach would require some kind of heat sink at sufficiently lower temperature such that when deflection occurs, the tip of the actuator touches the sink and cools down returning closer to its original non-deflected position where the cycle repeats. If the heat is being applied on the top surface of the anchor pad, simple cyclic operation may be achieved by either ceasing to apply the heat source or having the deflected tip of the actuator touching a structure connected to the cold substrate to release heat and start the cycle again.

Other possibilities include the use of flip-chip and precision microassembling techniques in a more elaborated microsystem comprising several mechanisms to transfer the energy from one component to another and obtain useful work. Some previously proposed micromechanisms that could apply the results being developed in this work include miniature Stirling engines researched by NASA, MEMS power generators, and other heat engines [14].

5. Simulations

To validate the results predicted by the analytical model, the single hot-arm thermal actuator was simulated using the commercial software ANSYS. The actuator is modeled using finite element modeling (FEM) while imposing thermal and mechanical boundary conditions as proposed in section 3. The material properties and parameters used for simulations are given in Table I and Table II.

TABLE I. MATERIAL PROPERTIES.

Material Properties	Value	Units
Density ρ	$2.2\text{x}10^{-15}$	$kg/\mu m^3$
Specific heat capacity c	$1\text{x}10^{+2}$	J/kg K
Thermal expansion α	4.7×10^{-6}	C^{-1}
Thermal conductivity of polysilicon k_p	148×10^{-6}	$W\mu m^{-1}C^{-1}$
Thermal conductivity of air k_v	26×10^{-9}	$W\mu m^{-1}C^{-1}$
Conductivity of Nitride k_n	2.25×10^{-6}	$W\mu m^{-1}C^{-1}$
Convection coefficient *h*	$5\text{x}10^{-12}$	$W/\mu m^2$ K

TABLE II. DIMENSIONS OF THE ACTUATOR.

Geometry	Value	Units
Length of first arm	210	μm
Length of second arm	210	μm
Width of first arm	2	μm
Width of second arm	2	μm
Gap	2	μm
Thickness of polysilicon	2	μm
Thickness of nitride	0.6	μm

Figure 8 shows the temperature distribution of the thermal actuator when a heat flux of $10W/cm^2$ is applied at one anchor pad.

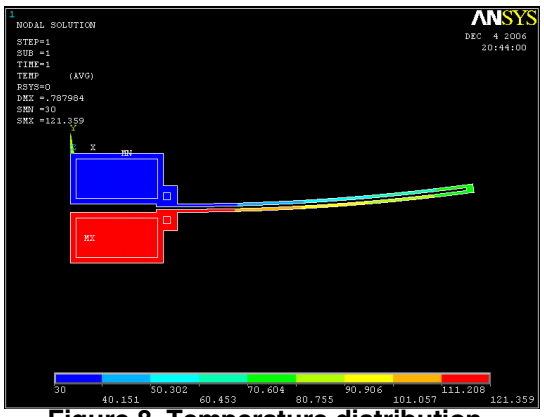

Figure 8. Temperature distribution.

Simulation results for the in-plane tip deflection of the actuator as a function of temperature are summarized in Figure 9.

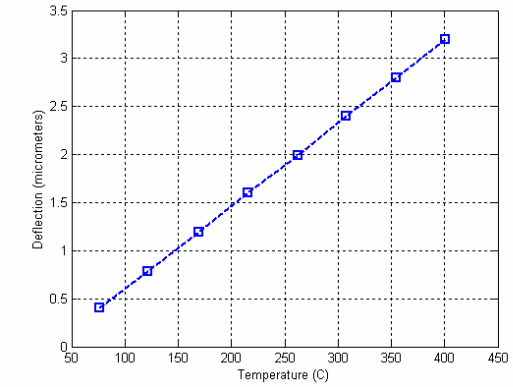

Figure 9. Maximum displacement of the actuator tip as a function of pad temperature.

6. Conclusion

An analytical model for externally heated thermal actuators was presented. The possibility of harvesting thermal energy already present in the environment opens the path for realizing autonomous micro-electro-mechanical systems eliminating the need of wiring to an external bulky battery or power supply unit. Furthermore, the power consumption and efficiency issues of traditional thermal actuators are not longer of concern if the energy is taken from waste heat coming out of an engine, a VLSI circuit, etc.

Finite element simulation results are in good agreement with those predicted by the mathematical models. This approach may be applied on the design and optimization of a variety of thermal actuators that exploit a thermal gradient in the surroundings and, eventually, on the development of complex heat engines capable of operating cyclically.

Preliminary results show that fairly large and useful displacements can be achieved at relatively low operating temperatures. However, only through fabrication one can truly understand the limits of the conceptual design and adjust the analytical models based on the actual test data. Accordingly, a number of test structures with different geometries have been submitted for fabrication using the standard Multi-User MEMS process (MUMPs).

7. References

[1] S.A. Jacobson and A.H. Epstein, An Informal Survey of Power MEMS, International Symposium on Micro-Mechanical Engineering, Dec. 2003.

[2] G. Hang and A. Lal, Self-reciprocating radioisotope-powered cantilever, Journal of Applied Physics, Vol. 92, No.2, pp 1122-1127, July 2002.

[3] D. Ryan and R. LaFollete, Power Supply and Energy Storage for Autonomous MEMS, Proc. of SAE Power Systems Conference, pp 359-363, November 2000.

[4] Huang Q. and Lee N., Analysis and design of polysilicon thermal flexure actuator, J. Micromech. Microeng. 9, 64-70, 1999.

[5] N.D. Mankame and G.K. Ananthasuresh, Comprehensive thermal modeling and characterization of an electro-thermal-compliant microactuator, J. Micromech. Microeng. 11 452-62, 2001.

[6] Yan D, Khajepour A and Mansour R, Modeling of two-hot-arm horizontal thermal actuator, J. Micromech. Microeng. 13 312–322, 2003.

[7] Yan D, Khajepour A and Mansour R, Design and Modeling of a MEMS bidirectional vertical thermal actuator, J. Micromech. Microeng. 14 841–850, 2004.

[8] B.L. Weaver et al., U.S. Patent 6,483,419, Nov. 2002.

[9] L. Que, J.-S. Park, and Y.B. Gianchandani, Bent-Beam Electrothermal Actuators - Part I: Single Beam and Cascaded Devices, Journal of Microelectromechanical Systems. vol. 10, no. 2, pp. 247-54, 2001.

[10] J. Carter et al., PolyMUMPS Design Handbook, MEMSCAP Inc., Revision 11.0, 2005.

[11] Fu H. et al., A One-Dimensional Model for Heat Transfer in Engine Exhaust Systems, SAE Technical Paper 2005-01-0696

[12] Cheng Y. et al., Thermal Analysis for Indirect Liquid Cooled MultiChip Module Using Computational Fluid Dynamic Simulation and Response Surface Methodology, IEEE Trans. Comp. Packag. Technol., vol. 29, no. 1, pp. 39-46, March 2006.

[13] C.JM. Lasance and R.E. Simons, Advances In High-Performance Cooling For Electronics, Electronics Cooling, November 2005, available on-line at: http://www.electronics-cooling.com/articles/2005/2005_nov_article2.php

[14] P.E. Clark et al., Small Power Technology Systems for Tetrahedral Rovers, American Institute of Physics Conference Proceedings, Vol. 813, pp. 889-897, Jan 2006.